Ma et al. Critical Care (2025) 29:354
https://doi.org/10.1186/s13054-025-05602-5

Critical Care

RESEARCH Open Access

Norepinephrine exacerbates LPS-induced cardiomyopathy via SIRT3/HO-1 axis-mediated ferroptosis

Dan Ma[1,3†], Weilun Fang[1,2†], Lei Cai[1], Wei Li[1] and Han Su[1*]

Abstract

Background Norepinephrine (NE) is a first-line vasopressor for patients with septic shock, and its overuse can lead to "catecholamine adverse effects", including cardiovascular diseases. Lipopolysaccharide (LPS)-induced cardiomyopathy is one of the leading causes of mortality in septic patients. Previous studies have revealed that catecholamine can accentuate LPS-induced cardiomyopathy, but the underlying mechanisms remain elusive.

Methods Adult mice and H9c2 cells were exposed to LPS and NE. Structural changes, cardiac function and LDH assays were measured to verify the synergistic effects of LPS and NE in vivo and in vitro. Inhibitors of ferroptosis, heme oxygenase-1 (HO-1) and an activator of SIRT3 were used to reverse the synergistic effects. 4-hydroxynonenal (4-HNE)/MDA assays, immunofluorescence, transmission electron microscopy (TEM) and western blotting were used to measure ferroptosis in this study.

Results In our study, conventional dosage of NE exacerbated LPS-induced cardiomyopathy in long term, followed by ferroptotic alternations of ferrous iron, reactive oxygen species (ROS), mitochondria shrinkage, lipid peroxidation and HO-1 expression. In addition, inhibition of ferroptosis suppressed cardiomyocyte death and cardiomyopathy induced by LPS and NE, indicating the critical contribution of ferroptosis to cardiac injury via the synergistic effects of NE and LPS. Our recent study identified SIRT3 as a therapeutic target for cardiac ferroptosis. In line with this, overexpression of SIRT3 alleviated the death of cardiomyocytes treated with NE + LPS, accompanied by attenuated ferroptosis and HO-1 level. Moreover, the suppression of HO-1 by zinc protoporphyrin (ZnPP) also attenuated ferroptosis in cardiomyocytes treated with NE and LPS.

Conclusion These data strongly indicate that long-term use of NE can further develop LPS-induced cardiomyopathy via SIRT3/HO-1 axis-mediated ferroptosis.

Keywords SIRT3, HO-1, Ferroptosis, Norepinephrine, LPS, Cardiomyopathy

†Dan Ma and Weilun Fang contributed equally to this work.

*Correspondence:
Han Su
603386@csu.edu.cn

Full list of author information is available at the end of the article

© The Author(s) 2025. **Open Access** This article is licensed under a Creative Commons Attribution-NonCommercial-NoDerivatives 4.0 International License, which permits any non-commercial use, sharing, distribution and reproduction in any medium or format, as long as you give appropriate credit to the original author(s) and the source, provide a link to the Creative Commons licence, and indicate if you modified the licensed material. You do not have permission under this licence to share adapted material derived from this article or parts of it. The images or other third party material in this article are included in the article's Creative Commons licence, unless indicated otherwise in a credit line to the material. If material is not included in the article's Creative Commons licence and your intended use is not permitted by statutory regulation or exceeds the permitted use, you will need to obtain permission directly from the copyright holder. To view a copy of this licence, visit http://creativecommons.org/licenses/by-nc-nd/4.0/.

SHOUT
SHARE
IT

Graphical abstract

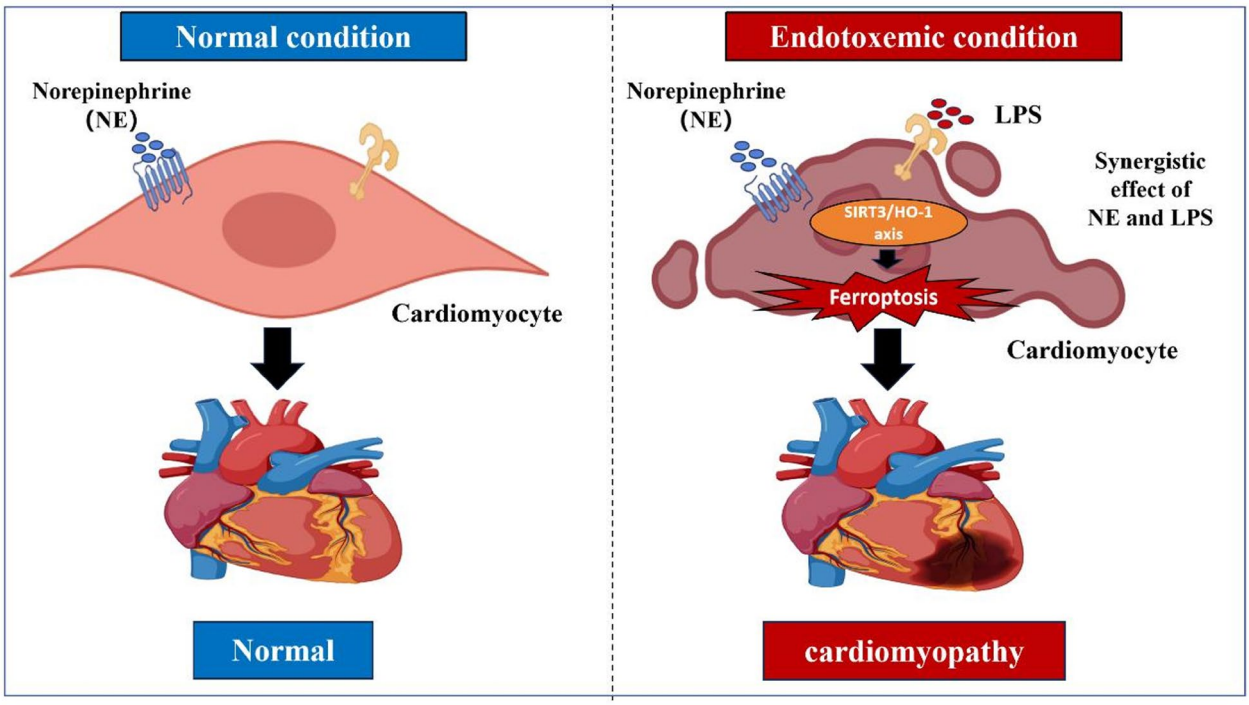

NE didn't result in myocardial impairment alone but could exacerbate LPS-induced cardiomyopathy via SIRT3/HO-1-mediated ferroptosis.

Introduction

Lipopolysaccharide (LPS)-induced endotoxemia could develop into septic shock which is a leading cause of death for septic patients. And vasopressor therapy is cornerstone treatment for patients with septic shock [1]. Among these vasopressors (most are catecholamines), norepinephrine (NE) is the first-line choice due to its ability to maintain both blood pressure and cardiac contractility by stimulating adrenergic receptors [1, 2]. Meanwhile, adverse effects such as suppressive inflammatory responses, increased lactate release and tissue damage emerge due to the overuse of catecholamines [3–5]. Cardiac dysfunction is one of the notable adverse effects of catecholamines in endotoxemia and sepsis, impairing circulatory dynamics and potentially increasing mortality [6–10]. More specifically, a recent study demonstrated that NE further increased chamber stiffness constant β and troponin T (TnT) levels in blood, suggesting that NE exacerbated myocardial injury in sepsis [11]. However, few studies fully illustrated its mechanisms. Only one study revealed that apoptosis contributes to catecholamine-exacerbated cardiac injuries in LPS-induced sepsis [9]. The role of other types of cell death in this condition remains elusive.

Latest research has shown that NE further increases cardiac oxygen consumption in sepsis [11], which augments oxidative stress and associated impairments consequently [12]. Ferroptosis functions importantly to septic cardiomyopathy [13], and it is tightly associated with oxidative stress [14]. However, the role of ferroptosis in NE-exacerbated LPS-induced cardiomyopathy needs further exploration. SIRT3, a critical regulator for mitochondrial deacetylation, mediates a series of molecular processes, including oxidative stress and associated cell death [15]. The protective function of SIRT3 in cardiovascular diseases has been fully clarified [16–20]. We recently proposed that SIRT3 is a newly identified regulator of ferroptosis [21, 22], and the functions of SIRT3/acetylated p53 axis in cardiac ferroptosis were further confirmed [23]. Moreover, heme oxygenase-1 is defined as a crucial mediator of ferroptosis due to its ability to degrade heme into ferrous iron. Its function in myocardial ferroptosis has been verified [24]. We previously reported the relationship between SIRT3 and HO-1 expression in kidney [25]. These data suggested the potential role of SIRT3/HO-1 axis in myocardial ferroptosis. Whereas, the association between the SIRT3/HO-1 axis and ferroptosis in NE-exacerbated LPS-induced cardiomyopathy is not clear.

In the present study, we aimed to explore the mechanisms for NE-exacerbated LPS-induced cardiomyopathy. Primarily, we found conventional dosage of NE in long term further developed cardiomyopathy and dysfunction in endotoxemia. Similarly, H9c2 cell death induced by LPS was also increased by NE. Furthermore, NE exacerbated ferroptotic changes induced by LPS in vivo and vitro, and inhibition of ferroptosis by ferrostanin-1 (Fer-1) significantly alleviated these synergistic alterations by NE and LPS. In addition, activation of SIRT3 (Ad-SIRT3 virus) and inhibition of HO-1 (ZnPP, zinc protoporphyrin) suppressed lipid peroxidation and increased ferrous iron levels in H9c2 cells treated with LPS and NE. Overall, these findings indicate the crucial role of SIRT3/HO-1 axis-mediated ferroptosis in NE-induced exacerbation of LPS-induced cardiomyopathy.

Materials and methods

Experimental animal model and treatment

C57BL/6 mice (8–12 weeks old) weighing 25–28 g were purchased from Hunan Slac Laboratory Animals Co. Ltd. (Changsha, Hunan, China). All animal experiments were approved by the Institutional Animal Care and Use Committee of Central South University. These mice were injected intraperitoneally with LPS (5 or 8 mg/ml). The mice were infused with NE (1–3 μg/kg/min) for 9 days via subcutaneously implanted Alzet miniosmotic pumps (Durect Corporation, Cupertino, CA, USA) while they were under anesthesia. The mice received an intraperitoneal injection of Fer-1 (2 mg/kg/d), 2-APQC (a SIRT3 activator, 30 mg/kg), disulfiram (DSF, pyroptosis inhibitor, 30 mg/kg), necrostatin-1 (Nec-1, necroptosis inhibitor, 1.5 mg/kg) (Fig. S1).

Cell culture and treatment

The H9c2 cell line was obtained from the Institute of Biochemistry and Cell Biology. H9c2 cells were cultured in standard DMEM (37 °C and 5% CO2). H9c2 cells were treated with LPS (200ng/ml), NE (50μM), ZnPP (HO-1 inhibitor, 2μM), DSF (10μM), Nec-1 (5 mM), Z-VAD-FMK (apoptosis inhibitor, 20μM), Fer-1 (2μM), C646 (p300 inhibitor, 3μM) or Oxyberberin (HO-1 activator, 30μM) for 24 h. Ad-SIRT3 virus (5μM) was added 6 h before stimulation.

Measurement of blood pressure

We measured mean arterial pressure (MAP) via tail-cuff occlusion method from manufacturer's instructions (Kent Scientific Corporation, Torrington, CT, USA). Measurements were taken at the same time each day. We took the first 2 days as an adjustment time for mice. Blood pressure measurements for remaining days were averaged for the final results.

Echocardiography

All groups of mice were subjected to transthoracic echocardiograms with a Vevo3100 Imaging System (VisualSonics Inc., Toronto, ON, Canada). We tested the ejection fraction (EF%) at 2, 4 and 7 days.

Histological and Immunofluorescence analysis

Neutral-buffered 10% formalin solution (SF93–20; Fisher Scientific, Pittsburgh, PA, USA) was used to store some of the tissues. Other parts were stored in frozen OCT compound (4585; Fisher Health Care, Houston, TX, USA). All tissues in formalin and OCT were cut at a thickness of 10 μm. Tissues in formalin solution were subjected to Masson's trichrome staining and hematoxylin & eosin (H&E) staining. The frozen parts were subjected to DHE staining. Images were acquired with a Nikon digital camera and a Nikon microscope and analyzed with Nikon software (Nikon, Tokyo, Japan). Six parts were selected in random. Images were analyzed via Image J (Bethesda, MD, USA).

Transmission electron microscopy (TEM)

Myocardial tissues and H9c2 cells were immersed in glutaraldehyde (2.5%) and fixed for 24 h (stored at 4 °C). Samples were washed with 0.1 M phosphate buffer and fixed in osmium for 2 h. Then we used phosphate buffer (0.1 M) to wash again. Alcohol and acetone were used to dehydrate these samples. After the dehydration, samples were immersed in penetrant A (acetone:812 = 2:1) for 2 h (37 °C) and penetrant B (acetone:812 = 1:2) overnight (37 °C). Samples were immersed in the embedding agent and placed in the mold with embedding agent. Then it was heated for 12 h (37 to 60 °C) and cut into Sects. (60–80 nm). Finally, the sections were immersed in uranium dioxychloride acetate solution for 1 h and lead citrate staining solution for 15 min. Images were observed and acquired digitally (JEM 1400, Japan).

Co-immunoprecipitation (Co-IP) assay

After intervention, the cells were lysed, homogenized, and centrifuged, the supernatant was taken. Monoclonal antibody (SIRT3) was added into the supernatant and incubated (4 °C) for 1 h. And protein G agarose was added and incubated (4 °C) for 4 h. After centrifuging, the immunization mixture was collected and tested for Western blot experiments (p300 and SIRT3 expression).

Western blot analysis

The protein concentrations were tested using a BCA protein assay kit (Pierce Co., Rockford, IL, USA). Equal amounts of protein were separated via SDS–PAGE and transferred to PVDF membranes. The PVDF membranes were blocked with milk and then incubated with primary antibodies overnight at 4 °C: α-smooth muscle

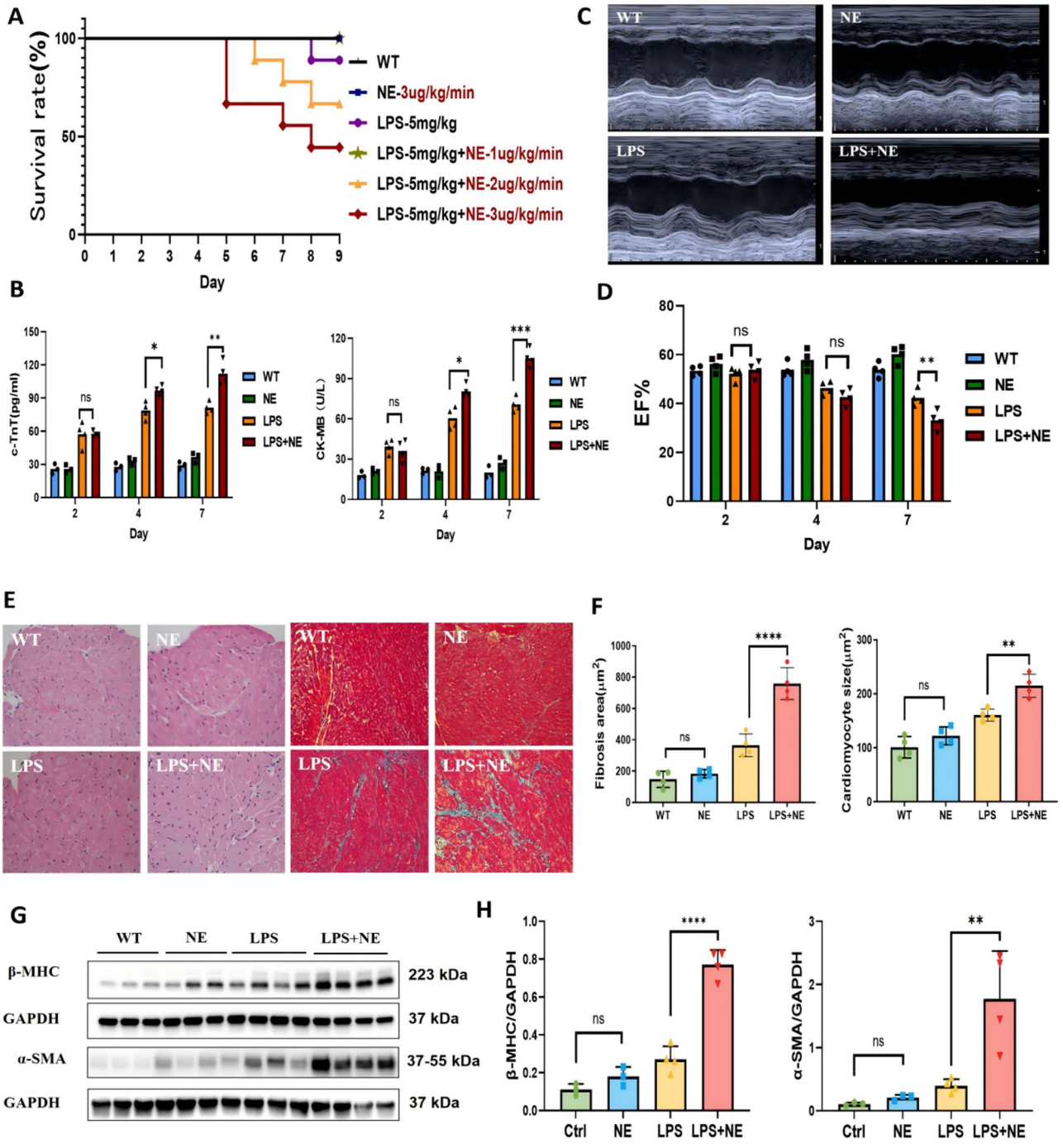

Fig. 1 NE further developed LPS-induced cardiomyopathy and cardiac dysfunction in long term **(A)** Survival rates of mice treated with LPS (5 mg/kg) and NE (1–3 μg/min/kg). **(B-D)** Quantification of c-TnT, CK-MB and EF% in the mice treated with LPS (5 mg/kg) and NE (2 μg/min/kg) after 2, 4 and 7 days ($n=4$). **(E)** Representative images of HE stained and Masson-stained heart sections from the mice treated with LPS (5 mg/kg) and NE (2 μg/min/kg) after 7 days ($n=3$). **(F)** Quantification of cardiomyocyte size and interstitial fibrosis area in the indicated groups ($n=3$). **(G, H)** Immunoblots and analysis of α-SMA, β-MHC and corresponding GAPDH in the indicated mouse hearts ($n=3$–4). Mean ± S.E.M., $^{**}p<0.01$, $^{***}p<0.001$, $^{****}p<0.0001$

actin (α-SMA), β-myosin heavy chain (β-MHC), p53 acetylation, 4-hydroxynonenal (4-HNE), p300, SIRT3 and heme oxygenase-1 (HO-1) (Abcam, Cambridge, MA, USA). After being washed with TBS-T, the PVDFs were incubated with secondary antibody (Cell Signaling Technology, Danvers, MA, USA), and the quality of the samples was determined via Bio-Rad (Hercules, CA, USA).

Cycloheximide (CHX) experiments

To measure HO-1 degradation, after 12 h stimulation of C646 (3μM) and Ad-SIRT3 virus (5μM), CHX (Sigma-Aldrich, 50 μg/ml) was added into H9c2 cells. After 0, 6 and 12 h incubation of CHX, protein was harvested tested by western blot.

Biochemical assays

The iron content in tissues and H9c2 cells was tested with an iron assay kit (Abcam). Serum NE, creatine kinase-MB and serum cTnT were tested via NE enzyme-linked immunosorbent assay kit (Alpco, USA), CK-MB assay kit (Biodiagnostic, Egypt) and MyBioSource ELISA kit. HO-1 and 4-HNE level were measured via HO-1 assay kit (Cusabio Biotech, USA) and 4-HNE assay kit (abcam).

Statistical analysis

The data are shown as the means ± S.E.M. We used one-way ANOVA to determine the significance of differences in the means of values among groups. The significance of differences between two groups was examined by Student's t test. $P < 0.05$ was considered statistically significant. The data were analyzed with Prism software, v.9.0.

Results

Conventional dosage of NE exacerbated LPS-induced cardiomyopathy

LPS impaired mean arterial pressure (MAP) of mice, and the doses of LPS is relevant to MAP negatively (Fig. S2A). To rescue impaired MAP of mice treated with LPS (5 and 8 mg/kg) to normal levels, 2 μg/kg/min was identified as conventional dose of NE (Fig. S2C, D). Notably, neither the conventional nor the high dose NE (2, 3 μg/kg/min) resulted in mortality when administered alone. However, the mortality rate was greater in those receiving both LPS and NE than that in the LPS group (Fig. 1A). Similarly, NE didn't cause cardiac injury alone but exacerbated increased blood levels of cTnT, CK-MB, cardiac hypertrophy, fibrosis and deteriorated ejection fraction (EF%), accompanied by increased expression of β-MHC and α-SMA (Fig. 1B-H).

Myocardial ferroptosis induced by LPS was accentuated by NE

Ferroptotic alterations in heart tissue, including reactive oxygen species (ROS), ferrous iron, mitochondrial shrinkage and 4-HNE expression in mice treated with LPS were further developed by NE (Fig. 2A-E, Fig. S5B). Similarly, LDH release, ferrous iron levels, ROS levels, expression of 4-HNE and mitochondrial shrinkage in H9c2 cells treated with LPS were further increased by NE treatment (Fig. 2F-K, Fig. S4A, S5A).

Inhibiting ferroptosis attenuated the NE-caused exacerbation of LPS-induced cardiomyopathy

Comparing to inhibitors of other cell death forms (Nec-1 for necroptosis, DSF for pyroptosis, Z-VAD-FMK for apoptosis), the increased LDH release induced by LPS and NE was most obviously mitigated by Fer-1, accompanied by decreased ROS levels (Fig. 3A-C). It was further confirmed in vivo that the suppression of ferroptosis alleviated mortality rate significantly compared to inhibiting pyroptosis and necroptosis (Fig. 4A). Improvement of EF% in the LPS + NE group by Fer-1 was better than by DSF (Fig. 4B). Correspondingly, there was significant attenuation of cardiac fibrosis and hypertrophy by Fer-1 compared to NE + LPS mice (Fig. 4C, D).

SIRT3/HO-1 axis-mediated myocardial ferroptosis induced by NE and LPS

The increased LDH release rate of H9c2 cells treated with LPS and NE was suppressed by Ad-SIRT3, followed by alleviation of ROS, ferrous iron and 4-HNE expression (Fig. 5A-F, Fig. S4B). Furthermore, the increased expression of HO-1 in the NE + LPS group was also diminished by Ad-SIRT3, indicating the regulatory role of SIRT3 in HO-1 levels. In addition, ferroptotic changes in LPS + NE group were reversed or accentuated by respectively inhibiting or activating HO-1 (Fig. 5A-F, Fig. S4B, Fig. S6). The overexpression of SIRT3 by 2-APQC improved cardiac remodeling in NE + LPS mice (Fig. 6A, B), accompanied with HO-1 expression and ferrous levels (Fig. 6C, D).

SIRT3 might regulates HO-1 stability via inhibiting p300

Previous study showed that p300, as a histone aetytranferase, contributes to HO-1 acetylation that affects HO-1 expression finally. Similarly, the enhanced expression of HO-1 in H9c2 cells treated with NE and LPS was diminished by C646 (p300 inhibitor). In addition, the expression of p300 in H9c2 cells was suppressed by Ad-SIRT3 and Co-IP assay indicated combination of SIRT3 and p300 (Fig. S3A-C). CHX degrades protein in certain time, which is used for testing protein degradation in different conditions. Our present study revealed that CHX degrade nearly 50% HO-1 expression within 12 h, while the degradation rate was significantly enhanced by overexpression of SIRT3 and inhibition of p300 (Fig. S3D, E).

Discussion

In the present study, we aimed to potential therapeutic target in NE-exacerbated LPS-induced cardiomyopathy. Primarily, we showed that NE accentuated cardiac injury and dysfunction induced by LPS, accompanied by ferroptosis in vivo and vitro. And inhibition of ferroptosis significantly ameliorated these impairments. Furthermore, we verified SIRT3 as a regulator of HO-1

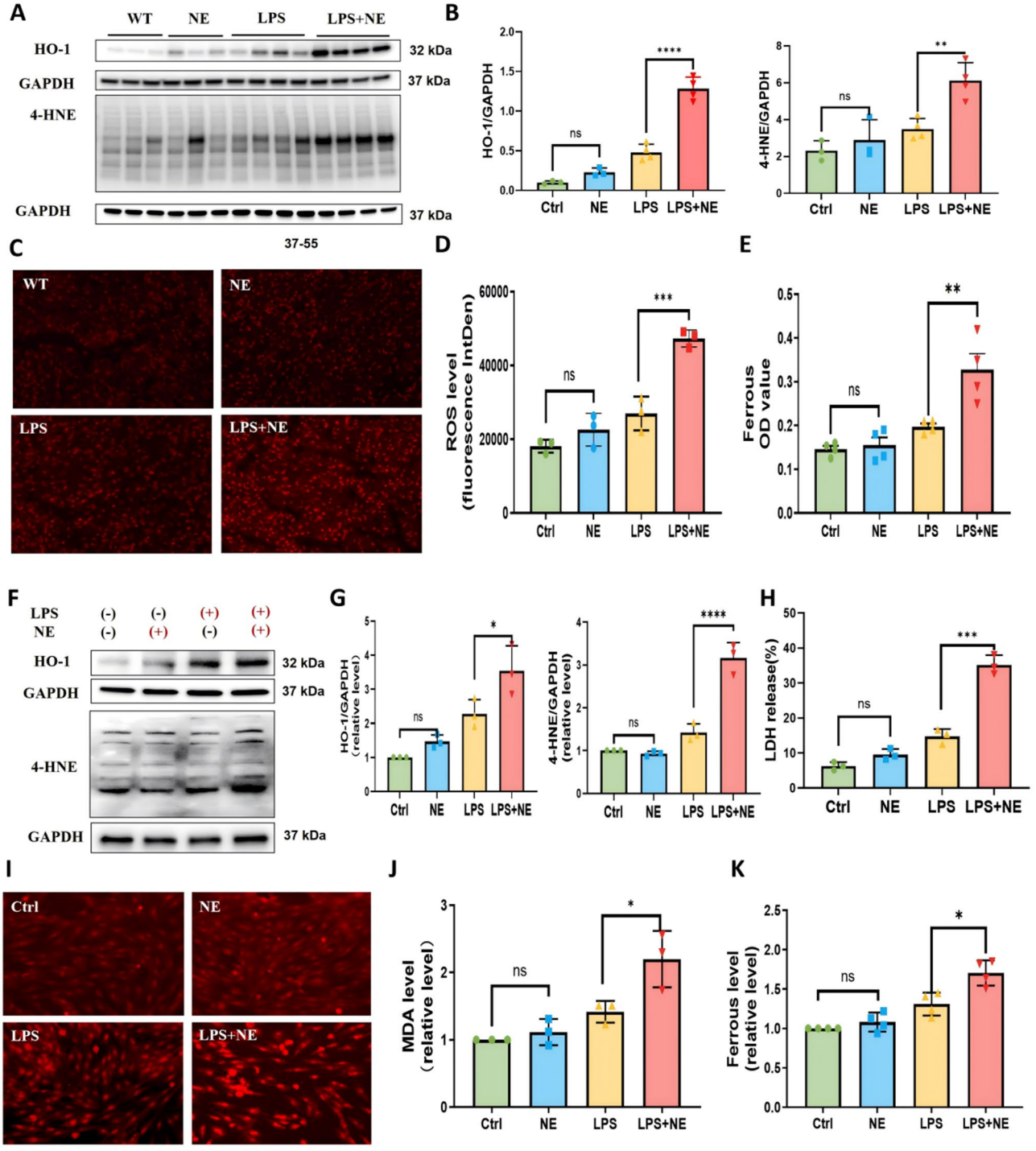

Fig. 2 NE exacerbated LPS-induced myocardial ferroptosis. **(A-B)** Immunoblots and analysis of HO-1, 4-HNE and corresponding GAPDH in the mice treated with LPS (5 mg/kg) and NE (2 μg/min/kg) after 7 days ($n = 3$). (**C**, **D)** Representative images and quantification of DHE staining in the indicated mouse hearts ($n = 3$). **(E)** Quantification of ferrous OD values in the indicated mouse hearts ($n = 3$). (**F**, **G)** Immunoblots and analysis of HO-1, 4-HNE and corresponding GAPDH in H9c2 cells treated with LPS (200ng/ml) or NE (50μM) for 24 h ($n = 3$). **(H)** LDH release rates in the indicated groups of H9c2 cells ($n = 3$). (**I**, **J)** Representative images and quantification of the integrated fluorescence density of DHE-stained H9c2 cells in the indicated groups ($n = 3$). **(K)** Quantification of ferrous OD values in the indicated H9c2 cells ($n = 3$). Mean ± S.E.M., $^{*}p < 0.05$, $^{**}p < 0.01$, $^{***}p < 0.001$, $^{****}p < 0.0001$

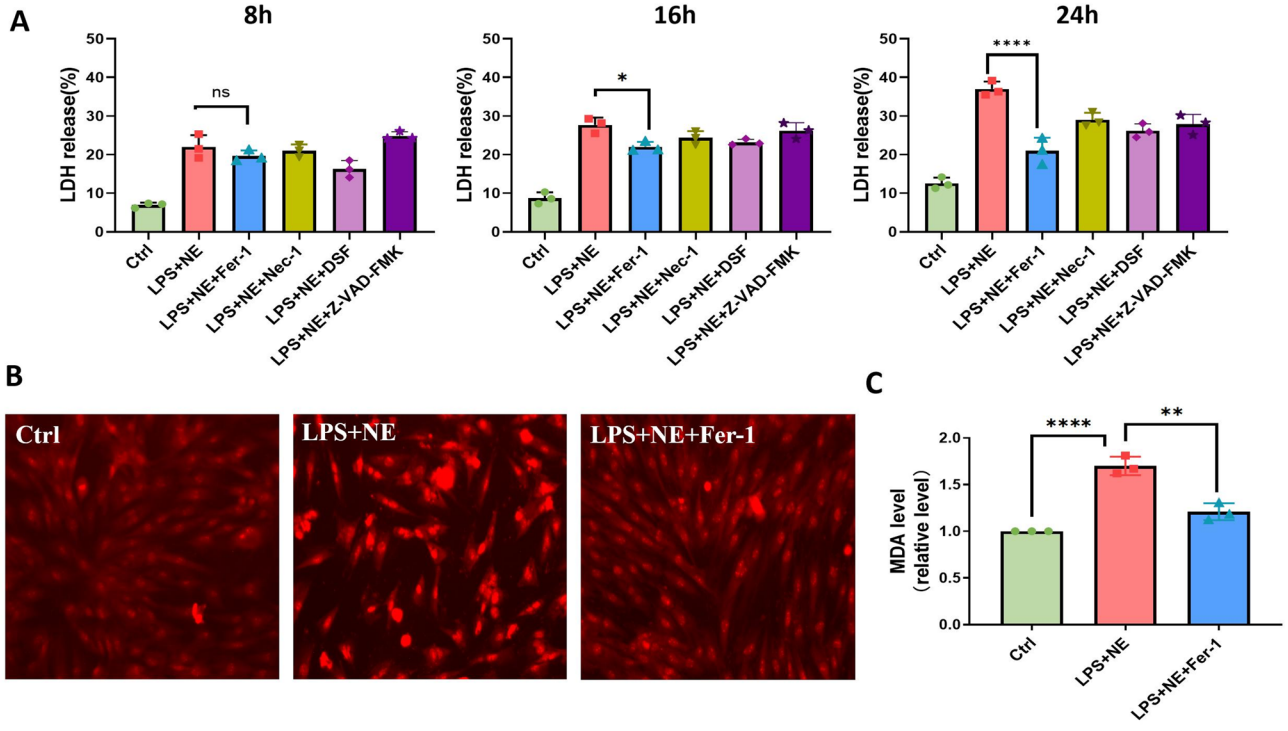

Fig. 3 Inhibiting ferroptosis in H9c2 cells significantly alleviated cell death at later time points. **(A)** Quantification of LDH release rates in H9c2 cells treated with LPS (200ng/ml), NE (50μM), Fer-1 (ferroptosis inhibitor, 2μM), Nec-1 (necroptosis inhibitor, 5 mM), DSF (pyroptosis inhibitor, 10μM) and Z-VAD-FMK (apoptosis inhibitor, 20μM) for 8, 16 and 24 h ($n=3$). **(B)** Representative images of DHE-stained H9c2 cells treated with LPS, NE or Fer-1 for 24 h ($n=3$). **(C)** Quantification of MDA in H9c2 cells treated with LPS, NE or Fer-1 for 24 h ($n=3$). Mean ± S.E.M., $^{*}p<0.05$, $^{**}p<0.01$, $^{***}p<0.001$, $^{****}p<0.0001$

in cardiomyocytes. And overexpressing SIRT3 and suppressing HO-1 alleviated the ferroptosis of cardiomyocytes. Taken together, our study indicated that SIRT3/HO-1 axis-mediated ferroptosis contributes to NE-exacerbated endotoxemia-induced cardiomyopathy.

For septic patients, norepinephrine is the first-line vasopressor used to guarantee stable blood pressure and organ perfusion [2]. Except exogenous NE, endogenous NE is largely secreted in sepsis due to sympathetic overactivation, causing surging of NE [5]. However, adverse effects like suppressed inflammatory responses, increased lactate release and tissue damage, emerge due to overuse of NE [3, 4, 26]. Cardiac dysfunction is one of the notable adverse effects and has recently attracted increasing attention [6–10]. Latest research revealed that continuing usage of NE accentuated chamber stiffness constant (β) and troponin-I (TnI) levels in blood of septic animal, followed by deteriorated left ventricular end-systolic volume (LVESV) representing potential systolic ability [11]. Deteriorated cardiac injury and dysfunction induce worsened blood pressure, resulting in increased mortality. Therefore, further investigations of the mechanisms could provide safer use of catecholamines for septic patients. Meanwhile, few studies illustrated its mechanisms comprehensively.

In this study, we used a two-hit model to mimic the clinical situation as much as possible. In order to study the synergistic effects of LPS and NE, appropriate dosage of LPS and NE need to be figured out. Our study revealed that the dosage of LPS is negatively associated with MAP. Compared to 3 and 8 mg/kg, 5 mg/kg of LPS is the lowest one inducing shock condition (MAP dropped nearly 20%) [27, 28], which is identified as the appropriate dosage in this study. Then we tried different dosage of NE (1–3 μg/min/kg). Guideline of sepsis (2021) proposed that we don't have to maintain MAP in normal levels [1], so the 3 μg/min/kg was relatively high. Compared to 1 μg/min/kg, 2 μg/min/kg revealed better performance in MAP alleviation. Thus 2 μg/min/kg was identified as conventional dosage in this study. Furthermore, NE (2 μg/min/kg) exacerbated mortality and cardiomyopathy compared to mice treated with LPS. But it didn't exhibit cardiotoxicity at early stage, evidenced by increased indicators associated with myocardial injury in serum at 4th day. In addition, exacerbated cardiac dysfunction occurred even later, followed by further accentuated cardiac remodeling. Meanwhile the deterioration of systolic dysfunction by NE didn't seem to be that obvious compared to structural impairments, which might be due to enhanced cardiac contractility via stimulating adrenergic receptors. These data suggested that the cardiotoxicity of

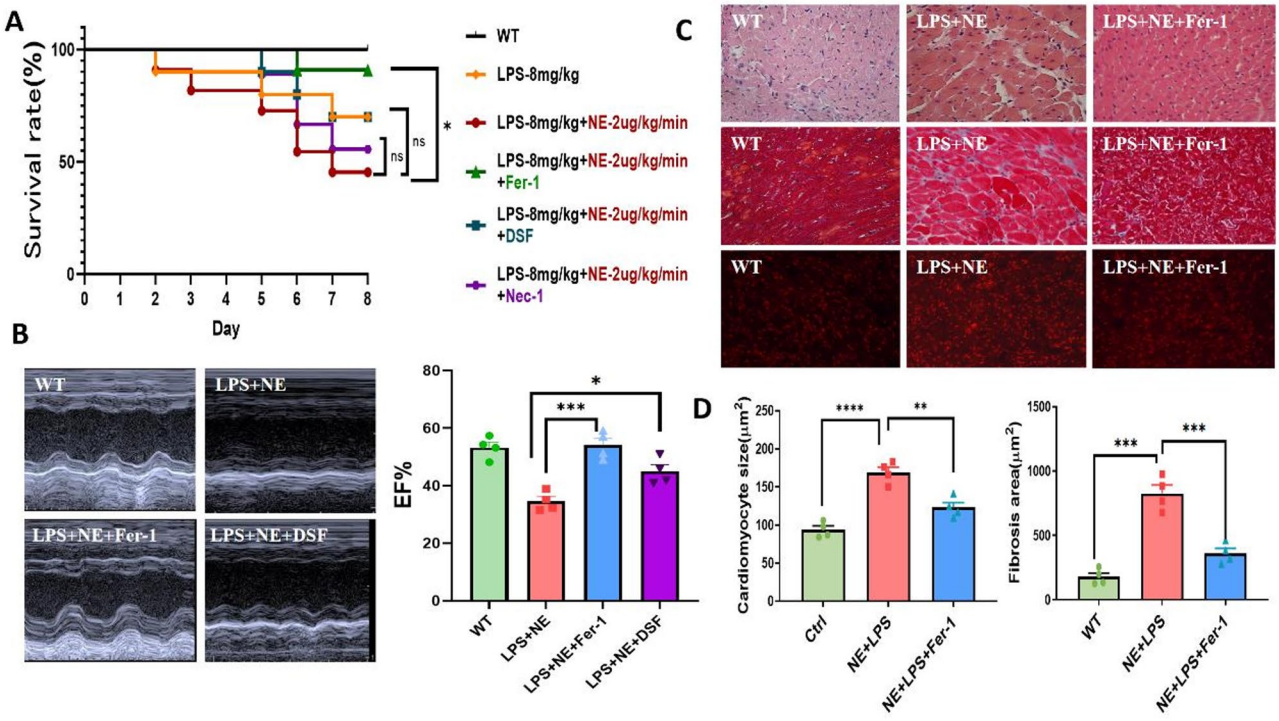

Fig. 4 Inhibition of ferroptosis rescued cardiac remodeling and dysfunction induced by the synergistic effects of LPS and NE. **(A)** Survival rates of mice treated with LPS (8 mg/kg), NE (2 μg/min/kg), Fer-1 (2 mg/kg/d), DSF (30 mg/kg) and Nec-1(1.5 mg/kg) ($n = 8$). **(B)** Representative images and analysis of cardiac function (EF%) after treatment with LPS (5 mg/kg), NE (2 μg/min/kg), Fer-1 (2 mg/kg/d) and DSF (30 mg/kg) for 7 days ($n = 4$). **C**, **D)** Representative images and quantification of HE-stained, Masson-stained and DHE-stained whole heart sections from mice treated with LPS (5 mg/kg), NE (2 μg/min/kg) or Fer-1 (2 mg/kg/d) for 7 days ($n = 3$). Mean ± S.E.M., $^{*}p < 0.05$, $^{**}p < 0.01$, $^{***}p < 0.001$, $^{****}p < 0.0001$

NE in LPS condition might be apparent when used for a long period of time. However, we still wondered whether these impairments resulted from overstimulation by NE. To answer this fundamental question, we 3 μg/min/kg doses NE to stimulate adrenergic receptors. But it didn't cause deteriorated cardiomyopathy and mortality alone. Overall, we are the first to propose that prolonged NE treatment exacerbates LPS-induced cardiomyopathy and associated dysfunction.

Cardiomyocyte death contributes crucially to cardiac injury [24]. But only recent study revealed apoptosis as a crucial death form in catecholamine-exacerbated LPS-induced cardiomyopathy [9]. The role of other forms of cell death remains elusive. Rising oxygen consumption is identified as a typical alteration in septic patients receiving NE treatment [29]. An authoritative study recently revealed that NE could greatly increase cardiac oxygen consumption in sepsis [11], suggesting that increased oxidative stress and corresponding cell death may occur [12]. Among diverse forms of cell death, ferroptosis is strongly correlated with oxidative stress since lipid peroxidation is its essential part [14]. However, whether ferroptosis functions importantly to NE-exacerbated LPS-induced cardiomyopathy is unknown. Our study demonstrated that typical alterations in ferroptosis, including lipid peroxidation and ferrous iron levels, were significantly increased by LPS. The infusion of NE did not lead to significant ferroptosis alone but further induced these ferroptotic changes in vivo and vitro. However, these ferroptotic changes did not support ferroptosis as a crucial form of cell death induced by the synergistic effects of LPS and NE. For further investigations, inhibitors of various types of cell death were used at different timepoints. Inhibitors of several main forms of cell death (apoptosis, necroptosis, pyroptosis and ferroptosis) were added to cardiomyocytes treated with LPS + NE previously. During the first 8 h, cardiomyocyte death induced by LPS and NE was reversed most effectively by blocking pyroptosis, which is consistent with the finding that NE exacerbated cardiac inflammation in sepsis [11]. However, at 24 h, the inhibition of ferroptosis was effectively alleviated, indicating that it contributes to the NE-induced exacerbation of cardiomyocyte death in endotoxemic condition at later stage. Moreover, compared to inhibition of pyroptosis and necroptosis, inhibition of ferroptosis induced the most significant alleviation in mortality and cardiac dysfunction induced by LPS and NE. Consistently, structural impairments were also reversed by Fer-1. These data confirmed the role of ferroptosis in the NE-induced exacerbation of myocardial injury in endotoxemia. Besides,

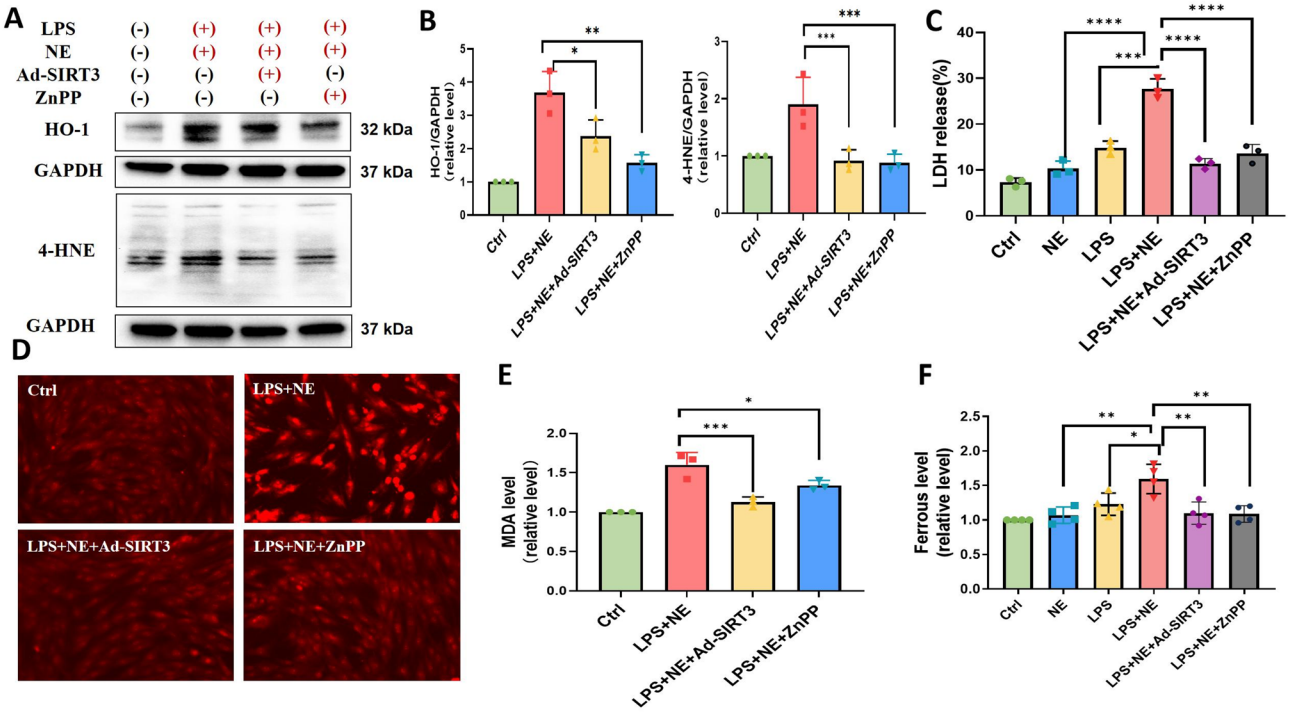

Fig. 5 Overexpression of SIRT3 and inhibition of HO-1 alleviated ferroptosis in H9c2 cells treated with LPS and NE. **(A, B)** Immunoblots and analysis of HO-1, 4-HNE and corresponding GAPDH in H9c2 cells treated with LPS (200ng/ml), NE (50μM), Ad-SIRT3 (a SIRT3 activator, 5μM) or ZnPP (a HO-1 inhibitor, 2μM) for 24 h ($n=3$). **(C)** LDH release rates in the indicated groups of H9c2 cells ($n=3$). **(D, E)** Representative images and quantification of the integrated fluorescence density of DHE-stained H9c2 cells in the indicated groups ($n=3$). **(F)** Quantification of ferrous OD values in the indicated H9c2 cells ($n=3$). Mean ± S.E.M., *$p<0.05$, **$p<0.01$, ***$p<0.001$, ****$p<0.0001$

lipid peroxidation, as the essential mechanism of ferroptosis, contributes to increased lactate production [30], which explain the accentuated lactate accumulation in heart [11]. Moreover, these findings offer potential therapeutic targets for corresponding cardiac impairments of endotoxemic or septic patients with NE treatment. However, its mechanisms need further exploration.

Iron overload contributes crucially to ferroptosis [24], and we are the first to report that cardiac ferrous iron accumulation induced by LPS was accentuated by NE. The source of increased ferrous iron needs further investigation. Heme oxygenase-1 is a key enzyme for heme degradation. Its overexpression results in overload of biliverdin, carbon monoxide and ferrous iron, which was identified as a canonical mechanism for ferroptosis [31]. In this study, similar to ferrous iron alterations, increased HO-1 expression induced by LPS was further promoted by NE. Meanwhile, HO-1 has been defined as an antioxidant factor in previous studies and plays a protective role in cardiovascular diseases [32]. Thus, the character of HO-1 in diverse diseases needs to be verified. In our study, we found that inhibition of HO-1 by ZnPP reversed the death of H9c2 cells induced by the synergistic effects of LPS and NE, followed by reversal of lipid peroxidation and ferrous iron levels. These data suggest that HO-1 contributes critically to the NE-exacerbated cardiomyocyte ferroptosis by regulating iron content.

SIRT3 is responsible for energy metabolism, balancing oxidative stress in mitochondria [15]. Recent studies have shown that the loss of SIRT3 contributes to ferroptosis via the regulation of iron levels in cancer cells and macrophages [33, 34]. Furthermore, our latest study demonstrated the emerging role of the SIRT3/acetylated p53 axis in myocardial ferroptosis. And we observed increased ferrous iron levels in the hearts of SIRT3KO mice [18, 23]. Whereas, acetylated p53 doesn't affect lipid peroxidation via iron overload [35]. The regulatory role of SIRT3 in ferroptosis via ferrous iron overload needs to be further clarified. Interestingly, our previous research revealed that knockout of SIRT3 increased HO-1 levels and iron overload in the kidney [25], indicating SIRT3/HO-1 axis as a potential regulator for ferrous iron in heart. In line with these findings, our present study revealed that lipid peroxidation and ferrous iron in cardiomyocytes treated with LPS + NE were significantly alleviated by activating SIRT3, accompanied by reduced HO-1 expression. This result was also verified via the use of 2-APQC (a small-molecule activator of SIRT3) in vivo [36]. We are the first one confirming the character of the SIRT3/HO-1 axis in the NE-induced exacerbation of myocardial ferroptosis caused by LPS. Moreover,

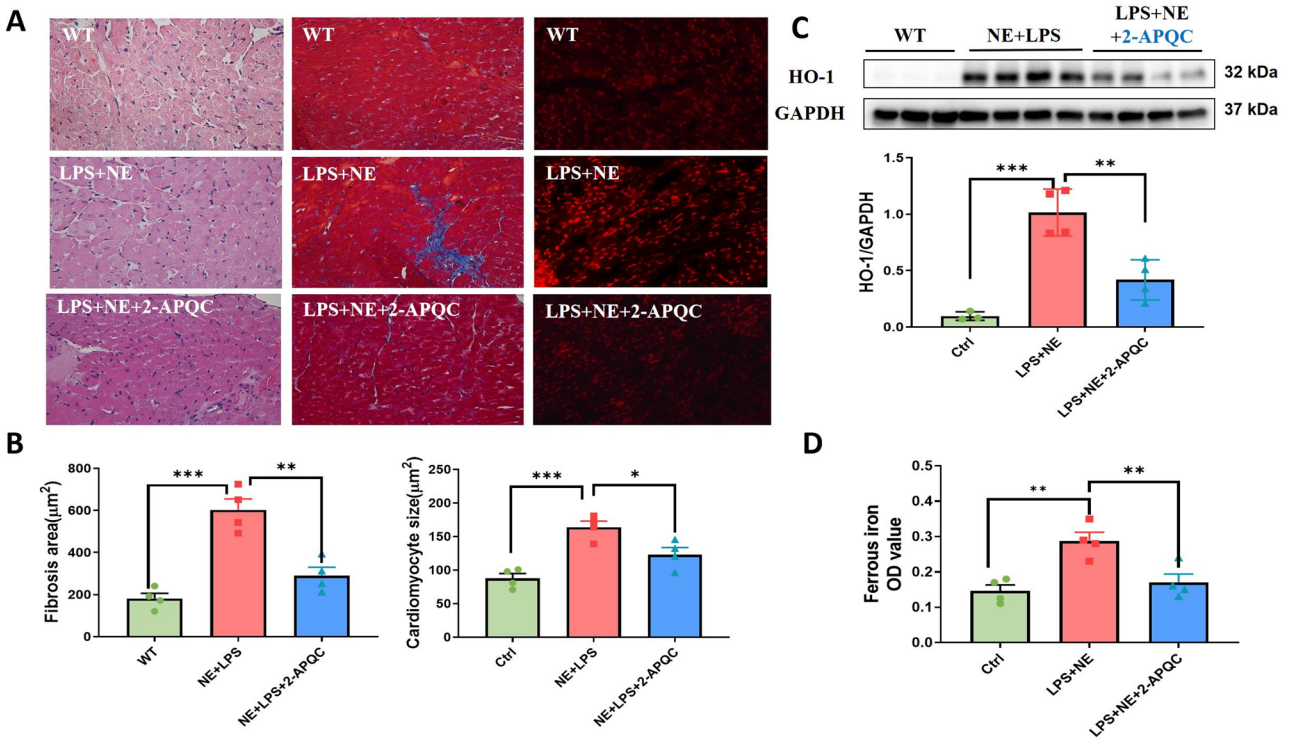

Fig. 6 Overexpression of SIRT3 via 2-APQC attenuated cardiomyopathy induced by the synergistic effects of LPS and NE. **(A)** Representative images of HE-stained, Masson-stained and DHE-stained whole heart sections from mice treated with LPS (5 mg/kg), NE (2 μg/min/kg) and 2-APQC (a SIRT3 activator, 30 mg/kg) for 7 days ($N=4$). **(B)** Quantification of cardiomyocyte size, interstitial fibrosis area and fluorescence integrated density in the DHE assay in the indicated groups ($n=4$). **(C)** Immunoblots and analysis of HO-1 and corresponding GAPDH in the indicated mouse hearts ($n=3$–4). **(D)** Quantification of ferrous OD values in the indicated mouse hearts ($n=4$). Mean ± S.E.M., *$p<0.05$, **$p<0.01$, ***$p<0.001$, ****$p<0.0001$

2-APQC, a newly identified SIRT3 activator, has been shown to rescue cardiac remodeling [36]. Our study also provides insight into the use of 2-APQC for alleviating cardiac injuries in septic patients with long-term NE treatment, which is highly valuable in clinic.

But how does SIRT3 affect HO-1 expression? A recent article demonstrated that acetylation by p300 is crucial for HO-1 levels [37]. In our study, we also observed inhibition of p300 reversed increased HO-1 expression in H9c2 cells induced by LPS and NE. Interestingly, we previously proposed SIRT3 as a regulator of p300 in heart [19], which was further evidenced by reduced p300 expression in H9c2 cells treated with Ad-SIRT3 in this study. Besides, CHX assay revealed that both Ad-SIRT3 and C646 enhanced degradation rate of HO-1 via deacetylation, indicating suppressed acetylation is responsible for the stability of HO-1. Therefore, SIRT3-inhibited p300 reduced acetylation of HO-1, which induces lower expression of HO-1 consequently.

Limitations

Animal model In this study we used LPS animal model to represent septic model. Meanwhile CLP is the most realistic method to mimic sepsis. Though LPS is a classic method for septic animal model as well, it is more closely to mimic endotoxemic condition in sepsis. In addition, NE infusion should be adjusted according to instant MAP, fixed dose and continuous NE infusion couldn't totally reflect clinical practice due to technical limitations at present.

Proposal of ferroptosis We chose ferroptosis mainly on the basis of a previous study revealing that increased oxygen consumption in septic heart was further promoted by NE. We only performed LDH assays, survival rate and cardiac function to identify ferroptosis as a crucial type of death. More evidences are needed to figure out the role of other cell death forms in NE-exacerbated LPS-induced cardiomyopathy.

Mechanism We identified SIRT3 might regulate HO-1 expression via p300 acetylation, which just suggested the pathway of NE-exacerbated myocardial ferroptosis induced by LPS. The specific process still needs further exploration.

Statistical issues Considering the "Reduction" principle of animal ethic, we tried to get effective data with lowest sacrifice. Thus the *n*-values were relatively small.

Conclusion

Overall, we systemically illustrate the adverse effects of NE in LPS-induced cardiomyopathy and proposed SIRT3/HO-1 axis-mediated ferroptosis as a potential therapeutic target for cardiotoxicity of NE in endotoxemia-induced sepsis. This study reminds us to observe cardiac dysfunction in septic patients receiving even conventional dosage of NE or other catecholamines in long term. Furthermore, we revealed the clinical value of treatment associated with the SIRT3/HO-1/ferroptosis axis (Fer-1, ZnPP and 2-APQC) in rescuing exacerbated cardiac dysfunction.

Abbreviations

α-SMA	α-smooth muscle actin
β-MHC	β-myosin heavy chain
CK-MB	Creatine kinase-MB isoenzyme
Co-IP	Co-immunoprecipitation
DSF	Disulfiram
EF	Ejection fraction
Fer-1	Ferrostatin-1
H&E	Hematoxylin and eosin
4-HNE	4-hydroxynonenal
HO-1	Heme oxygenase-1
LDH	Lactate dehydrogenase
LPS	Lipopolysaccharide
NE	Norepinephrine
Nec-1	Necrostatin-1
ROS	Reactive oxygen species
SIRT3	Sirtuin3
TEM	Transmission electron microscopy
TnT	Troponin T
ZnPP	Zinc protoporphyrin

Supplementary Information

The online version contains supplementary material available at https://doi.org/10.1186/s13054-025-05602-5.

Supplementary Material 1.

Supplementary Material 2.

Acknowledgements

We acknowledge Prof. Liangliang Fan and Yingjie Tan for providing thoughtful ideas for the study at beginning.

Author contributions

H. Su designed the research; W. Li, L. Cai, D. Ma and W. Fang contributed thoughtful comments; D. Ma and W. Fang performed the research; H. Su and D. Ma analyzed the data; W. Fang and H. Su wrote and edited the manuscript; and all the authors have read and approved the final manuscript.

Funding

This study was supported by grants from the National Natural Science Foundation of China (82400577), the Natural Science Foundation of Hunan Province (2023JJ40904) and the China Postdoctoral Science Foundation (2024M753691).

Data availability

Data is provided within the manuscript or supplementary information files.

Declarations

Ethics approval

All animal experiments were approved by the Institutional Animal Care and Use Committee of Central South University.

Competing interests

The authors declare no competing interests.

Author details

[1]Department of General Surgery, The Third Xiangya Hospital, Central South University, 138# Tongzipo Road, Changsha 410013, Hunan, China
[2]Department of Oncology, The Third Xiangya Hospital, Central South University, Changsha, Hunan, China
[3]Department of Obstetrics and Gynecology, Hunan Provincial Maternal and Child Health Care Hospital, Changsha, Hunan, China

Received: 23 April 2025 / Accepted: 2 August 2025
Published online: 13 August 2025

References

1. Evans L, Rhodes A, Alhazzani W, Antonelli M, Coopersmith CM, French C, Machado FR, McIntyre L, Ostermann M, Prescott HC, et al. Surviving sepsis campaign: international guidelines for management of sepsis and septic shock 2021. Intensive Care Med. 2021;47(11):1181–247.
2. De Backer D, Biston P, Devriendt J, Madl C, Chochrad D, Aldecoa C, Brasseur A, Defrance P, Gottignies P, Vincent JL. Comparison of dopamine and norepinephrine in the treatment of shock. N Engl J Med. 2010;362(9):779–89.
3. Andreis DT, Singer M. Catecholamines for inflammatory shock: a Jekyll-and-Hyde conundrum. Intensive Care Med. 2016;42(9):1387–97.
4. Laterre PF, Berry SM, Blemings A, Carlsen JE, François B, Graves T, Jacobsen K, Lewis RJ, Opal SM, Perner A, et al. Effect of selepressin vs placebo on ventilator- and vasopressor-free days in patients with septic shock: the SEPSIS-ACT randomized clinical trial. JAMA. 2019;322(15):1476–85.
5. Singer M. Catecholamine treatment for shock–equally good or bad? Lancet. 2007;370(9588):636–7.
6. Wilkman E, Kaukonen KM, Pettilä V, Kuitunen A, Varpula M. Association between inotrope treatment and 90-day mortality in patients with septic shock. Acta Anaesthesiol Scand. 2013;57(4):431–42.
7. Yang D, Dai X, Xing Y, Tang X, Yang G, Harrison AG, Cahoon J, Li H, Lv X, Yu X, et al. Intrinsic cardiac adrenergic cells contribute to LPS-induced myocardial dysfunction. Commun Biol. 2022;5(1):96.
8. Hollenberg SM. Understanding stress cardiomyopathy. Intensive Care Med. 2016;42(3):432–5.
9. Wang Y, Wang Y, Yang D, Yu X, Li H, Lv X, Lu D, Wang H. β_1-adrenoceptor stimulation promotes LPS-induced cardiomyocyte apoptosis through activating PKA and enhancing camkii and IκBα phosphorylation. Crit Care. 2015;19(1):76.
10. Domizi R, Calcinaro S, Harris S, Beilstein C, Boerma C, Chiche JD, D'Egidio A, Damiani E, Donati A, Koetsier PM, et al. Relationship between norepinephrine dose, tachycardia and outcome in septic shock: A multicentre evaluation. J Crit Care. 2020;57:185–90.
11. Garcia B, Su F, Dewachter L, Favory R, Khaldi A, Moiroux-Sahraoui A, Annoni F, Vasques-Nóvoa F, Rocha-Oliveira E, Roncon-Albuquerque R, editors. Myocardial effects of angiotensin II compared to norepinephrine in an animal model of septic shock. Crit Care. 2022;26(1):281.
12. Shadel GS, Horvath TL. Mitochondrial ROS signaling in organismal homeostasis. Cell. 2015;163(3):560–9.
13. Liu C, Zou Q, Tang H, Liu J, Zhang S, Fan C, Zhang J, Liu R, Liu Y, Liu R, et al. Melanin nanoparticles alleviate sepsis-induced myocardial injury by suppressing ferroptosis and inflammation. Bioact Mater. 2023;24:313–21.
14. Stockwell BR, Friedmann Angeli JP, Bayir H, Bush AI, Conrad M, Dixon SJ, Fulda S, Gascón S, Hatzios SK, Kagan VE, et al. Ferroptosis: a regulated cell death nexus linking metabolism, redox biology, and disease. Cell. 2017;171(2):273–85.
15. Li L, Zeng H, He X, Chen JX. Sirtuin 3 alleviates diabetic cardiomyopathy by regulating TIGAR and cardiomyocyte metabolism. J Am Heart Assoc. 2021;10(5): e018913.
16. He X, Cantrell AC, Williams QA, Gu W, Chen Y, Chen JX, Zeng H. p53 acetylation exerts critical roles in pressure overload-induced coronary microvascular

dysfunction and heart failure in mice. Arterioscler Thromb Vasc Biol. 2024;44(4):826–42.
17. Chen JX, Li L, Cantrell AC, Williams QA, Zeng H. High glucose activates prolyl hydroxylases and disrupts HIF-α signaling via the P53/TIGAR pathway in cardiomyocyte. Cells. 2023;12(7):1060. https://doi.org/10.3390/cells12071060
18. Cantrell AC, Besanson J, Williams Q, Hoang N, Edwards K, Bishop GR, Chen Y, Zeng H, Chen JX. Ferrostatin-1 specifically targets mitochondrial iron-sulfur clusters and aconitase to improve cardiac function in Sirtuin 3 cardiomyocyte knockout mice. J Mol Cell Cardiol. 2024;192:36–47.
19. Su H, Zeng H, He X, Zhu SH, Chen JX. Histone acetyltransferase p300 inhibitor improves coronary flow reserve in SIRT3 (sirtuin 3) knockout mice. J Am Heart Assoc. 2020;9(18): e017176.
20. Su H, Zeng H, Liu B, Chen JX. Sirtuin 3 is essential for hypertension-induced cardiac fibrosis via mediating pericyte transition. J Cell Mol Med. 2020;24(14):8057–68.
21. Liu L, Li Y, Cao D, Qiu S, Li Y, Jiang C, Bian R, Yang Y, Li L, Li X, et al. Sirt3 inhibits gallbladder cancer by induction of AKT-dependent ferroptosis and blockade of epithelial-mesenchymal transition. Cancer Lett. 2021;510:93–104.
22. Zhu J, Sun R, Sun K, Yan C, Jiang J, Kong F, Shi J. The deubiquitinase USP11 ameliorates intervertebral disc degeneration by regulating oxidative stress-induced ferroptosis via deubiquitinating and stabilizing Sirt3. Redox Biol. 2023;62: 102707.
23. Su H, Cantrell AC, Chen JX, Gu W, Zeng H. SIRT3 deficiency enhances ferroptosis and promotes cardiac fibrosis via p53 acetylation. Cells. 2023;12(10):1428. https://doi.org/10.3390/cells12101428
24. Fang X, Wang H, Han D, Xie E, Yang X, Wei J, Gu S, Gao F, Zhu N, Yin X, et al. Ferroptosis as a target for protection against cardiomyopathy. Proc Natl Acad Sci U S A. 2019;116(7):2672–80.
25. Feng X, Su H, He X, Chen JX, Zeng H. SIRT3 deficiency sensitizes Angiotensin-II-induced renal fibrosis. Cells. 2020;9(11):2510. https://doi.org/10.3390/cells9112510
26. Anantasit N, Boyd JH, Walley KR, Russell JA. Serious adverse events associated with vasopressin and norepinephrine infusion in septic shock. Crit Care Med. 2014;42(8):1812–20.
27. van de Sandt AM, Windler R, Gödecke A, Ohlig J, Zander S, Reinartz M, Graf J, van Faassen EE, Rassaf T, Schrader J, et al. Endothelial NOS (NOS3) impairs myocardial function in developing sepsis. Basic Res Cardiol. 2013;108(2):330.
28. Cai J, Lu S, Yao Z, Deng YP, Zhang LD, Yu JW, Ren GF, Shen FM, Jiang GJ. Glibenclamide attenuates myocardial injury by lipopolysaccharides in streptozotocin-induced diabetic mice. Cardiovasc Diabetol. 2014;13:106.
29. de Montmollin E, Aboab J, Mansart A, Annane D. Bench-to-bedside review: Beta-adrenergic modulation in sepsis. Crit Care. 2009;13(5):230.
30. Soares AF, Guichardant M, Cozzone D, Bernoud-Hubac N, Bouzaïdi-Tiali N, Lagarde M, Géloën A. Effects of oxidative stress on adiponectin secretion and lactate production in 3T3-L1 adipocytes. Free Radic Biol Med. 2005;38(7):882–9.
31. Luo P, Liu D, Zhang Q, Yang F, Wong YK, Xia F, Zhang J, Chen J, Tian Y, Yang C, et al. Celastrol induces ferroptosis in activated HSCs to ameliorate hepatic fibrosis via targeting Peroxiredoxins and HO-1. Acta Pharm Sin B. 2022;12(5):2300–14.
32. Ryter SW. Heme oxgenase-1, a cardinal modulator of regulated cell death and inflammation. Cells. 2021;10(3):515. https://doi.org/10.3390/cells10030515
33. Jeong SM, Lee J, Finley LW, Schmidt PJ, Fleming MD, Haigis MC. SIRT3 regulates cellular iron metabolism and cancer growth by repressing iron regulatory protein 1. Oncogene. 2015;34(16):2115–24.
34. Gao J, Huang C, Kong L, Zhou W, Sun M, Wei T, Shen W. SIRT3 regulates clearance of apoptotic cardiomyocytes by deacetylating frataxin. Circ Res. 2023;133(7):631–47.
35. Liu Y, Gu W. P53 in ferroptosis regulation: the new weapon for the old guardian. Cell Death Differ. 2022;29(5):895–910.
36. Peng F, Liao M, Jin W, Liu W, Li Z, Fan Z, Zou L, Chen S, Zhu L, Zhao Q, et al. 2-APQC, a small-molecule activator of Sirtuin-3 (SIRT3), alleviates myocardial hypertrophy and fibrosis by regulating mitochondrial homeostasis. Signal Transduct Target Ther. 2024;9(1): 133.
37. Hsu FF, Chiang MT, Li FA, Yeh CT, Lee WH, Chau LY. Acetylation is essential for nuclear heme oxygenase-1-enhanced tumor growth and invasiveness. Oncogene. 2017;36(49):6805–14.

Publisher's note

Springer Nature remains neutral with regard to jurisdictional claims in published maps and institutional affiliations.